

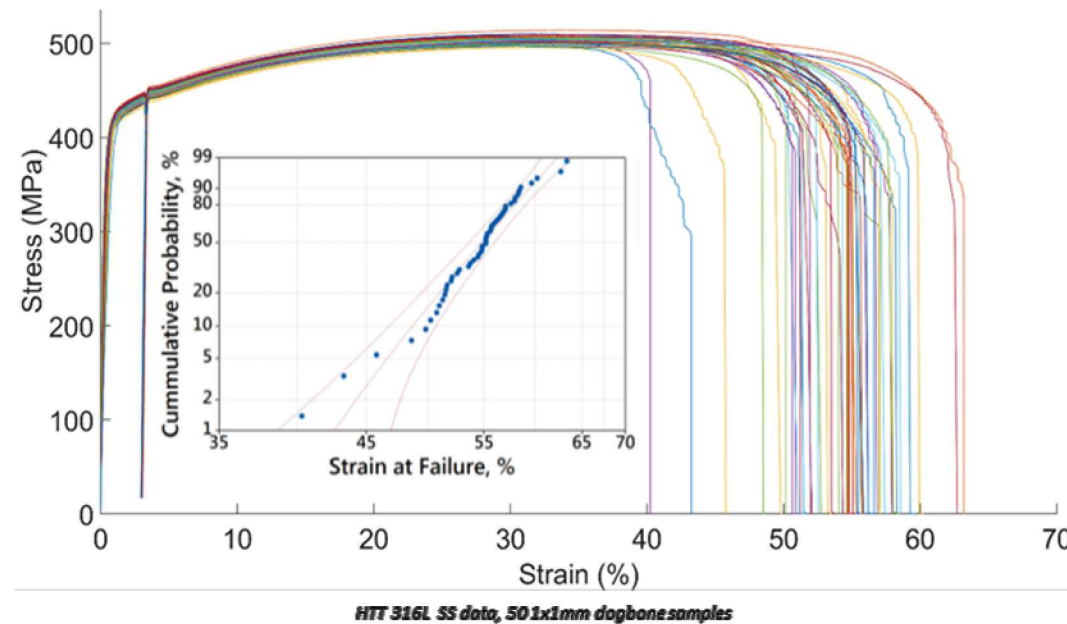
Metal Powder Feedstock Reuse in Additive Manufacturing: Characterization of 316L Stainless Steel

Michael Heiden, Jeff Rodelas, Lisa Deibler, Josh Koepke, Dan Tung, David Saiz, Bradley Jared
Sandia National Laboratories, Albuquerque, NM

Solid Freeform Fabrication 2018, Austin, TX
August 13-15th, 2008

Motivation for study on powder reuse

- Currently 5-46% of cost in PBF is feedstock; reuse reduces costs¹
- 50-90% of the build area is unused powder¹
- Still relatively unknown how heat-affected powders change and affect part properties
- Variability in mechanical properties may partially be due to quality of feedstock

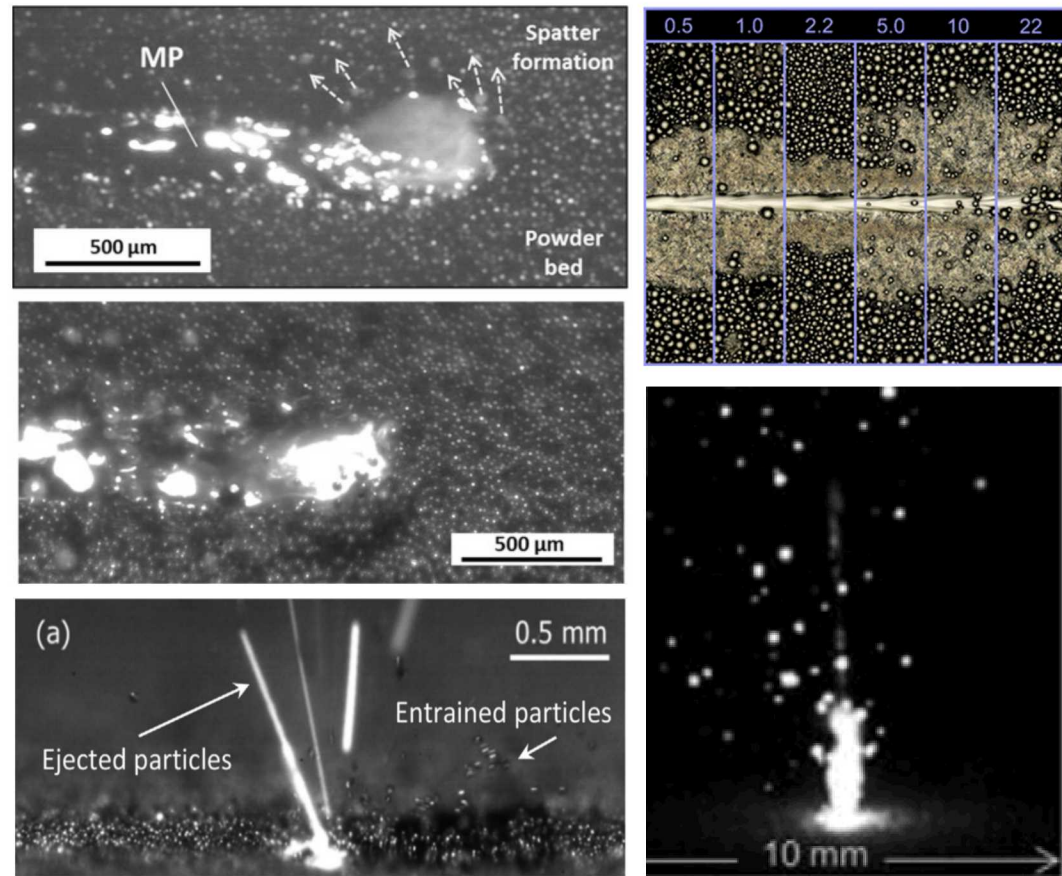


To improve reusability/recyclability of powders, this study aims to determine:

- How does the energy source degrade feedstock quality?
- How do particle properties affect variability in final part properties?

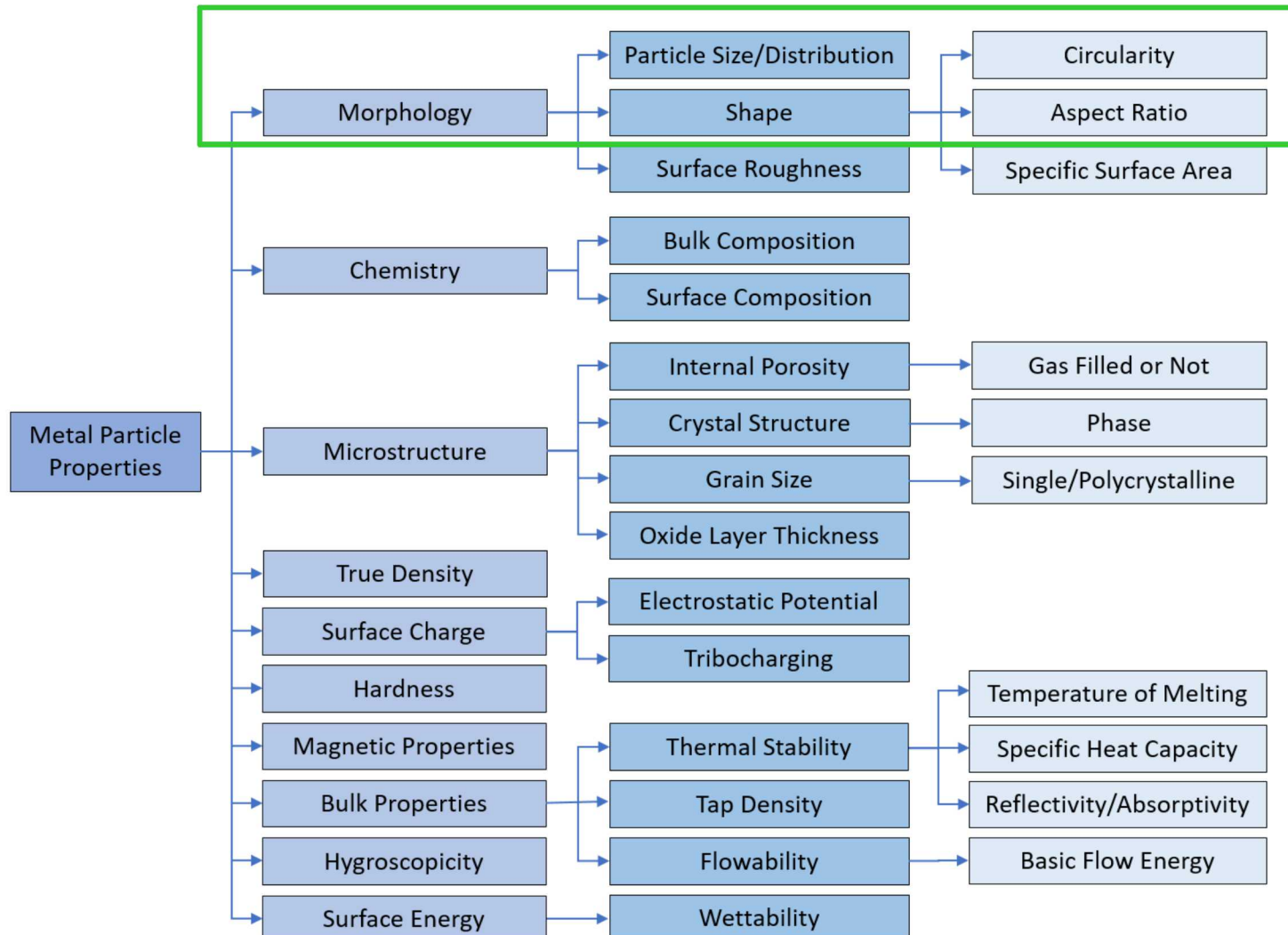
Dynamic SLM laser-powder interactions

- Vaporization of alloy species
- Particle fusion near weld pool
- Particle collisions
- Melt pool ejecta/spatter
- Gas entrainment of nearby particles
- Denudation
- Satellite formation
- Clusters/agglomerates



Need to understand powder reuse effects → apply characterization technique suite to understand attribute changes as a function of reuse

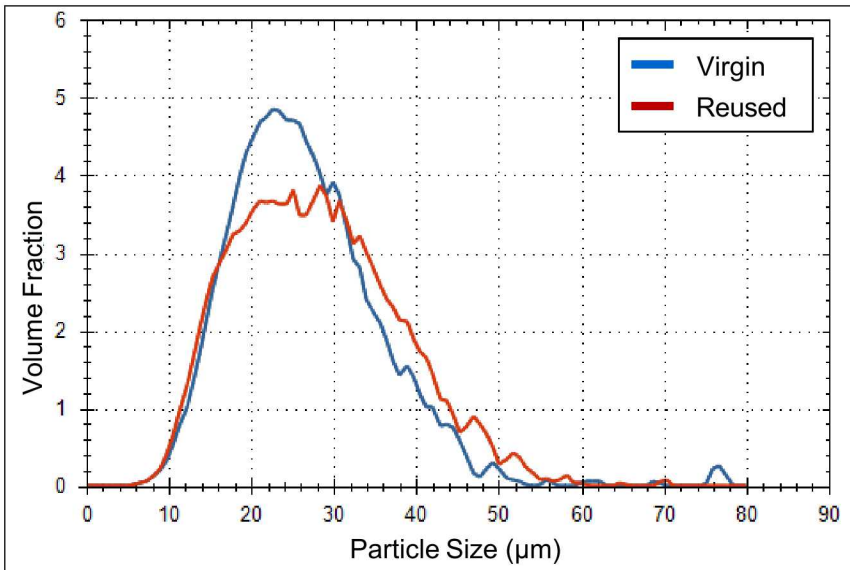
Outline – 316L characterization



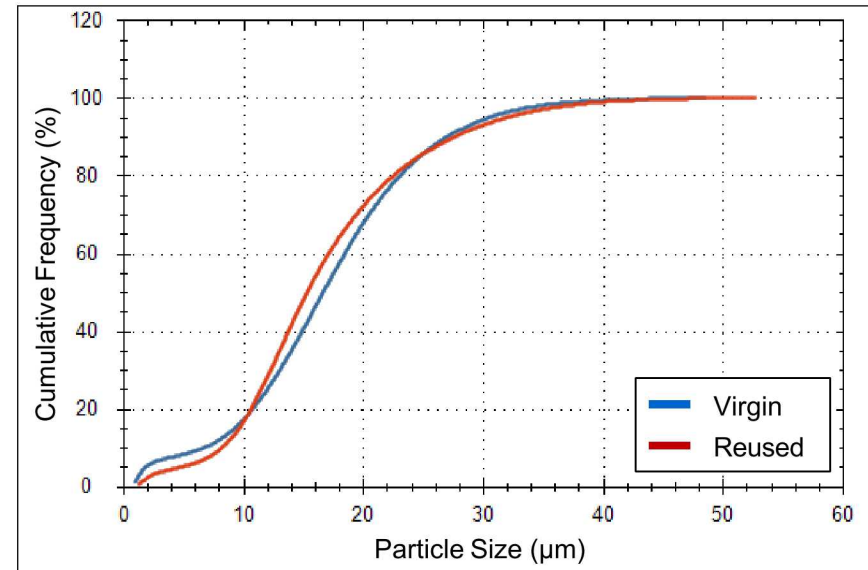
- Each powder batch was sieved between multiple build cycles, with a total 'reuse' of 30 times

No major change to PSD with 30 reuses

Differential Size Distribution



Cumulative Size Distribution



(based on cumulative number frequency)

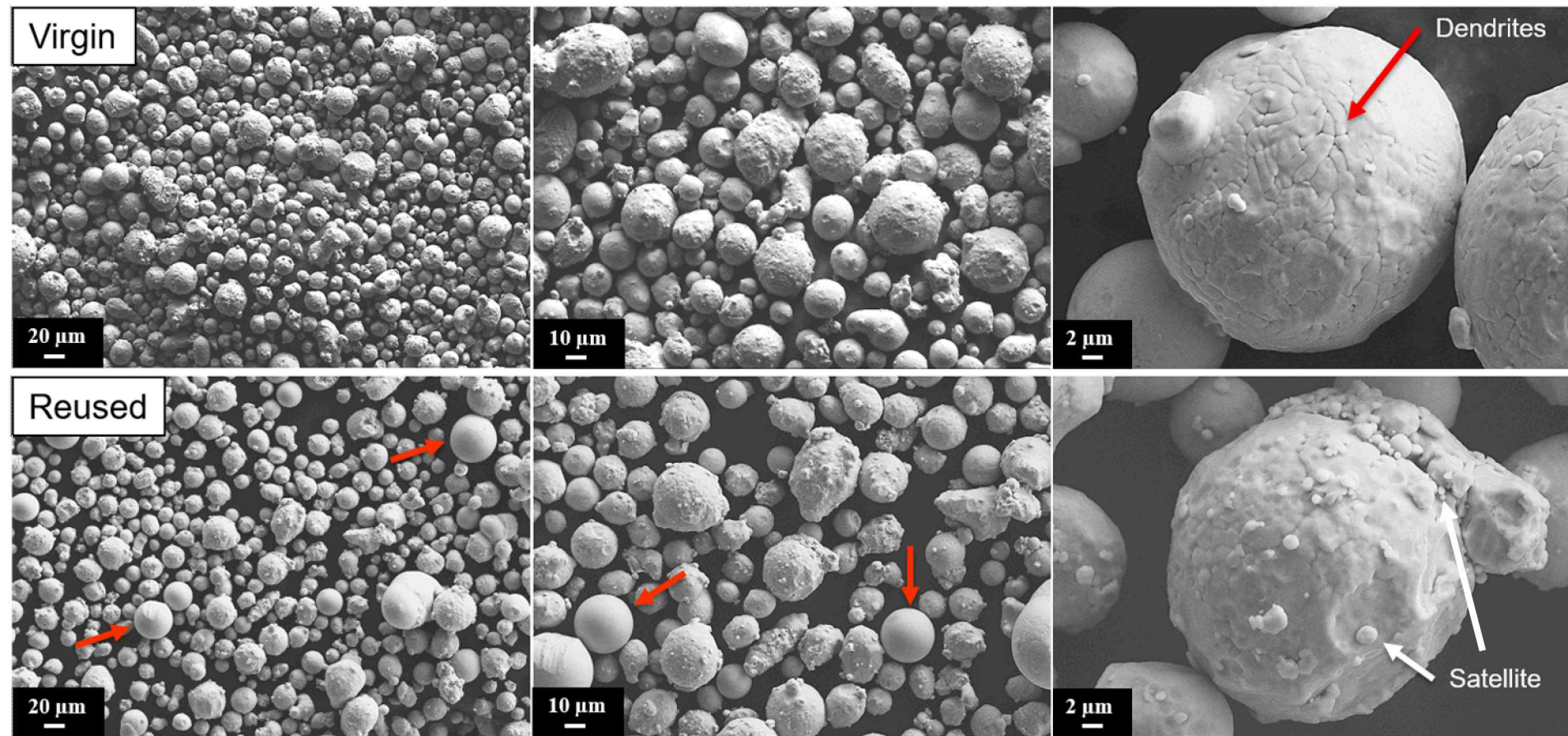
Powder (Stdev)	Average Dia. (μm)	D _n 10 (μm)	D _n 50 (μm)	D _n 90 (μm)	Aspect Ratio	Circularity
Virgin	16.4 (1.7)	7.0 (3.3)	16.9 (2.9)	26.9 (2.2)	0.68 (0.04)	0.83 (0.07)
Reused	16.9 (1.2)	8.2 (1.3)	15.4 (1.0)	27.5 (2.2)	0.66 (0.05)	0.81 (0.08)

(based on volume fraction)

Powder (Stdev)	Average Dia. (μm)	D _v 10 (μm)	D _v 50 (μm)	D _v 90 (μm)		
Virgin	22.4 (0.2)	13.6 (0.1)	21.1 (0.2)	32.7 (0.4)	-	-
Reused	35.7 (3.1)	17.2 (1.1)	27.1 (0.5)	59.3 (16.9)	-	-

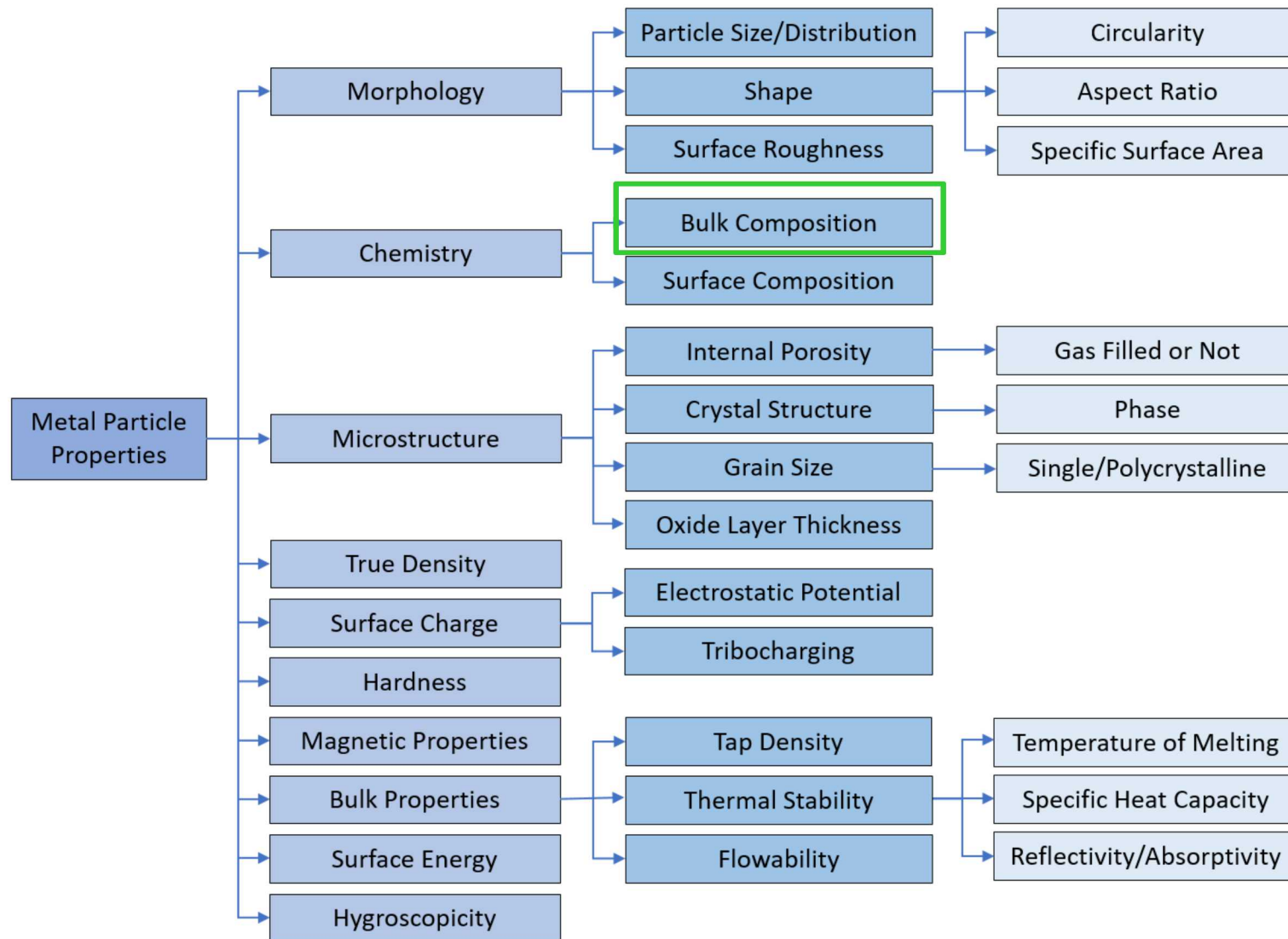
- Particle size distribution shifts right
- Reduction in fine particles (<10 μm)
- Slight increase in amount of larger particles
- Wider particle distribution (volume fraction) with reuse

Satellites, agglomeration, and smooth particles



- Reused powder has significantly more satellite formation and agglomerates
- Reused contains substantial amount of highly spherical particles
- Can view solidification substructure on each virgin particle, not always for reused

Outline – Bulk composition analysis



No major changes to powder bulk composition

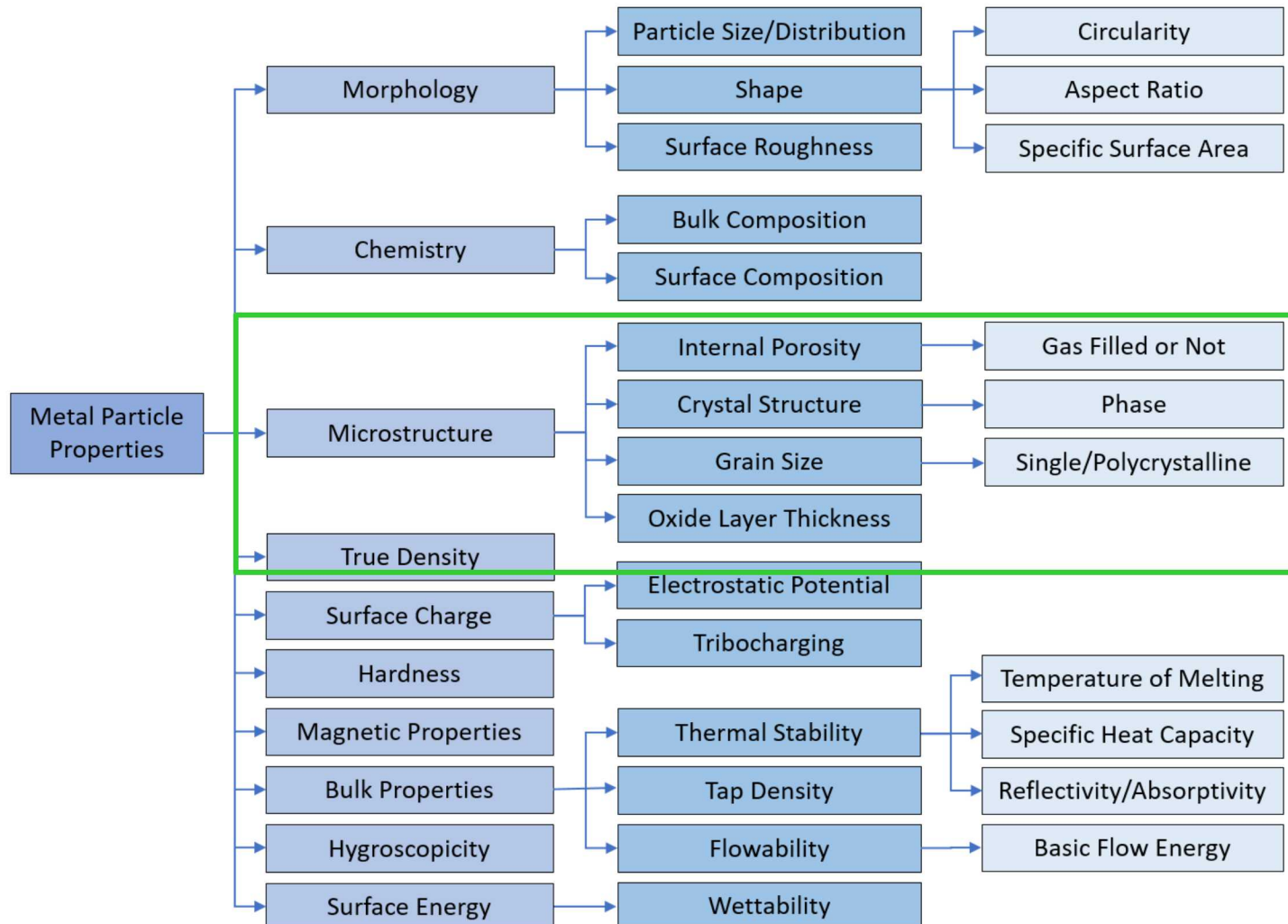


ICP-MS analysis

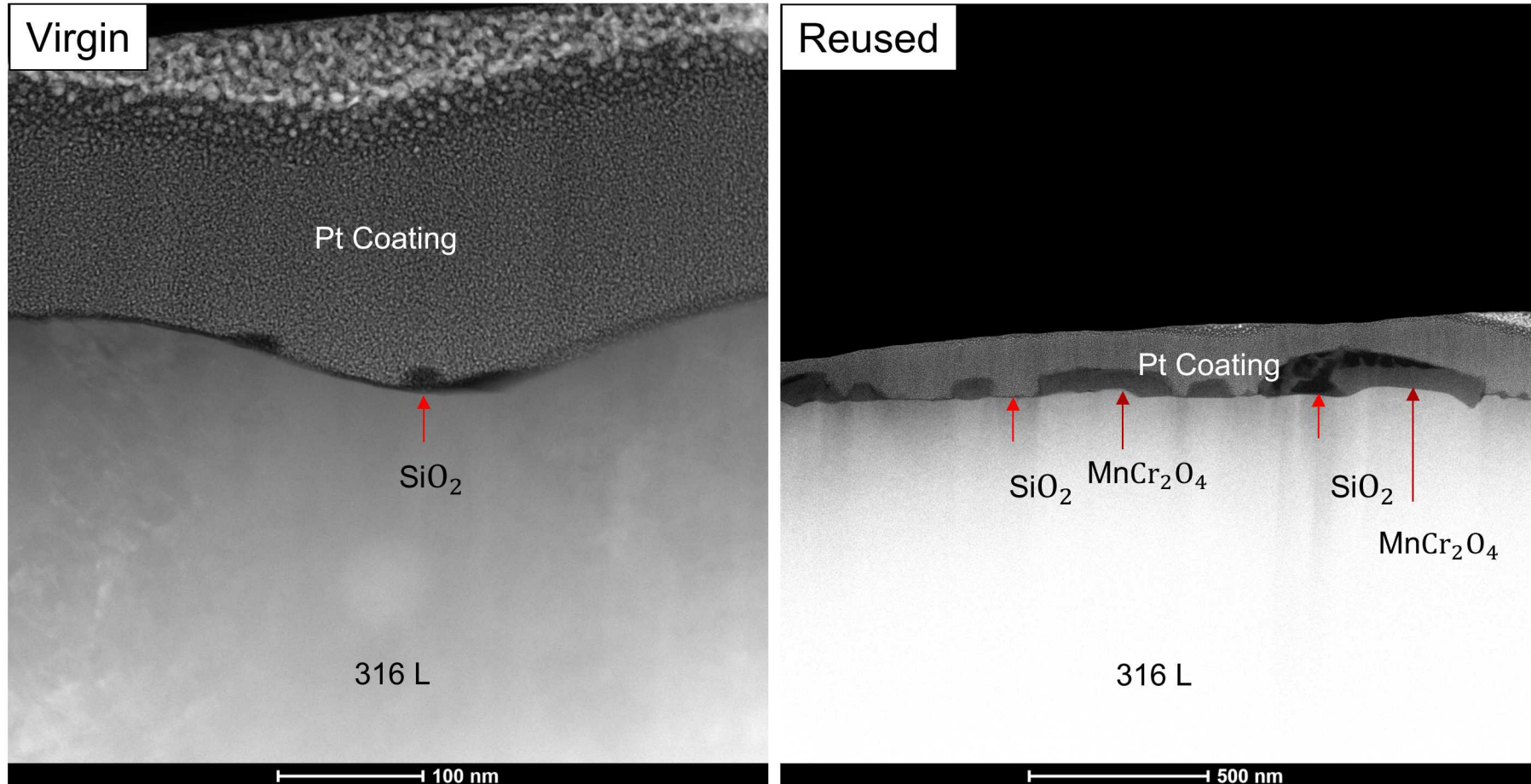
Wt.% (Stdev)	Fe	Cr	Ni	Mo	Si	Mn	Cu	P	Co	C	S	O	N
Virgin	67.8 (0.3)	16.84 (0.34)	10.81 (0.22)	2.05 (0.20)	0.65 (0.10)	1.20 (0.12)	0.21 (0.03)	0.015 (0.002)	0.098 (0.015)	0.011 (0.002)	0.014 (0.002)	0.067 (0.010)	0.086 (0.013)
Reused	67.6 (0.3)	16.91 (0.34)	10.90 (0.22)	2.02 (0.20)	0.60 (0.09)	1.27 (0.13)	0.22 (0.03)	0.016 (0.002)	0.11 (0.016)	0.016 (0.002)	0.014 (0.002)	0.095 (0.014)	0.090 (0.013)
ASTM Spec [2]	61-69	16-18	10-14	2-3	1 max	2 max	-	0.045 max	-	0.03 max	0.03 max	-	-

- O and C increased slightly with 30 reuses
- Differences for other elements within measurement uncertainty range
- All compositions within governing ASTM spec

Outline – Microstructural changes



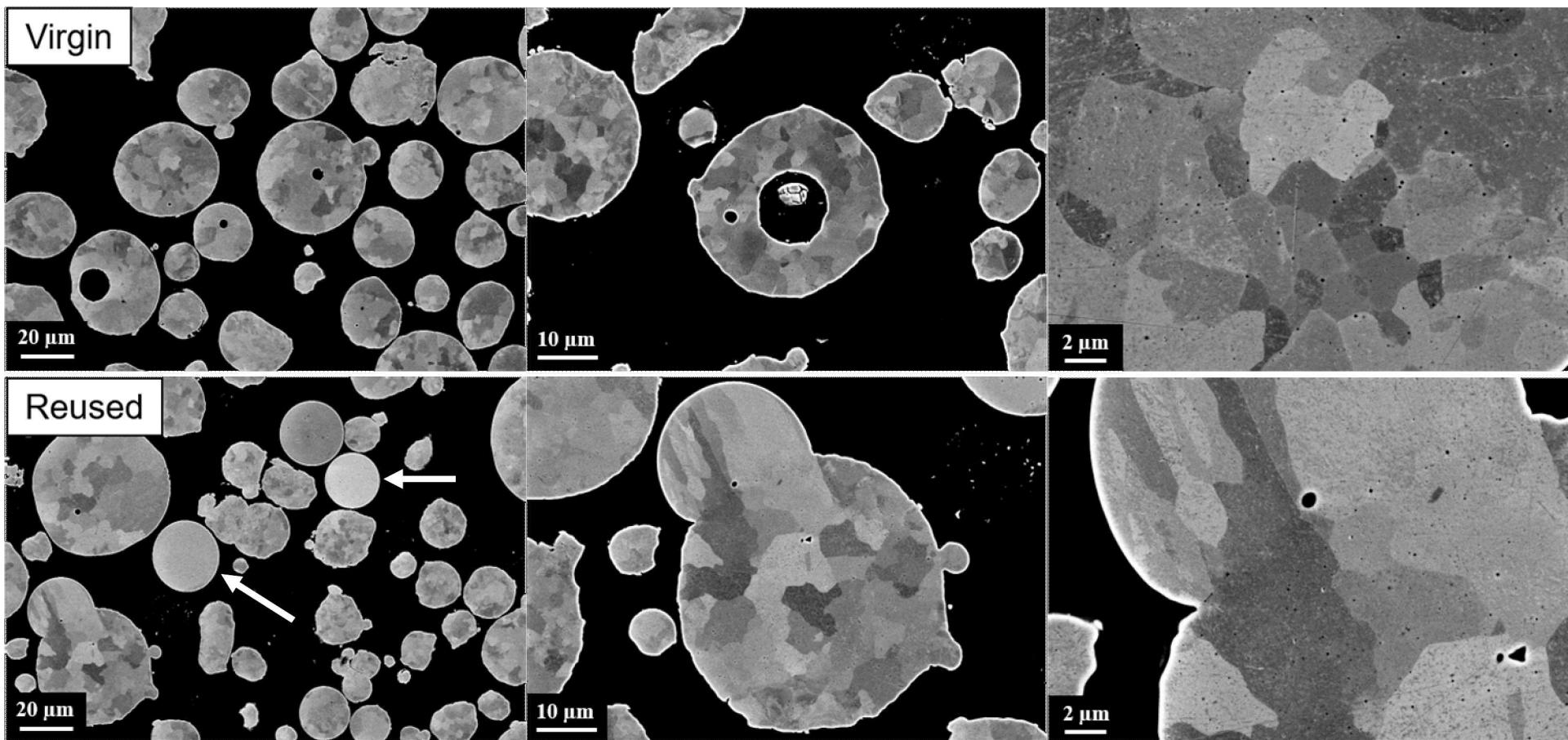
TEM shows increased oxide thickness with reuse



Oxide Layer	Virgin	Virgin Nodules	Reused	Reused Nodules
Average (nm)	3.7	14.8	4.4	79.5
Stdev (nm)	0.5	2.6	1.1	30.1

- Reuse generates oxide nodules across particle surface, which eventually grows into full layer

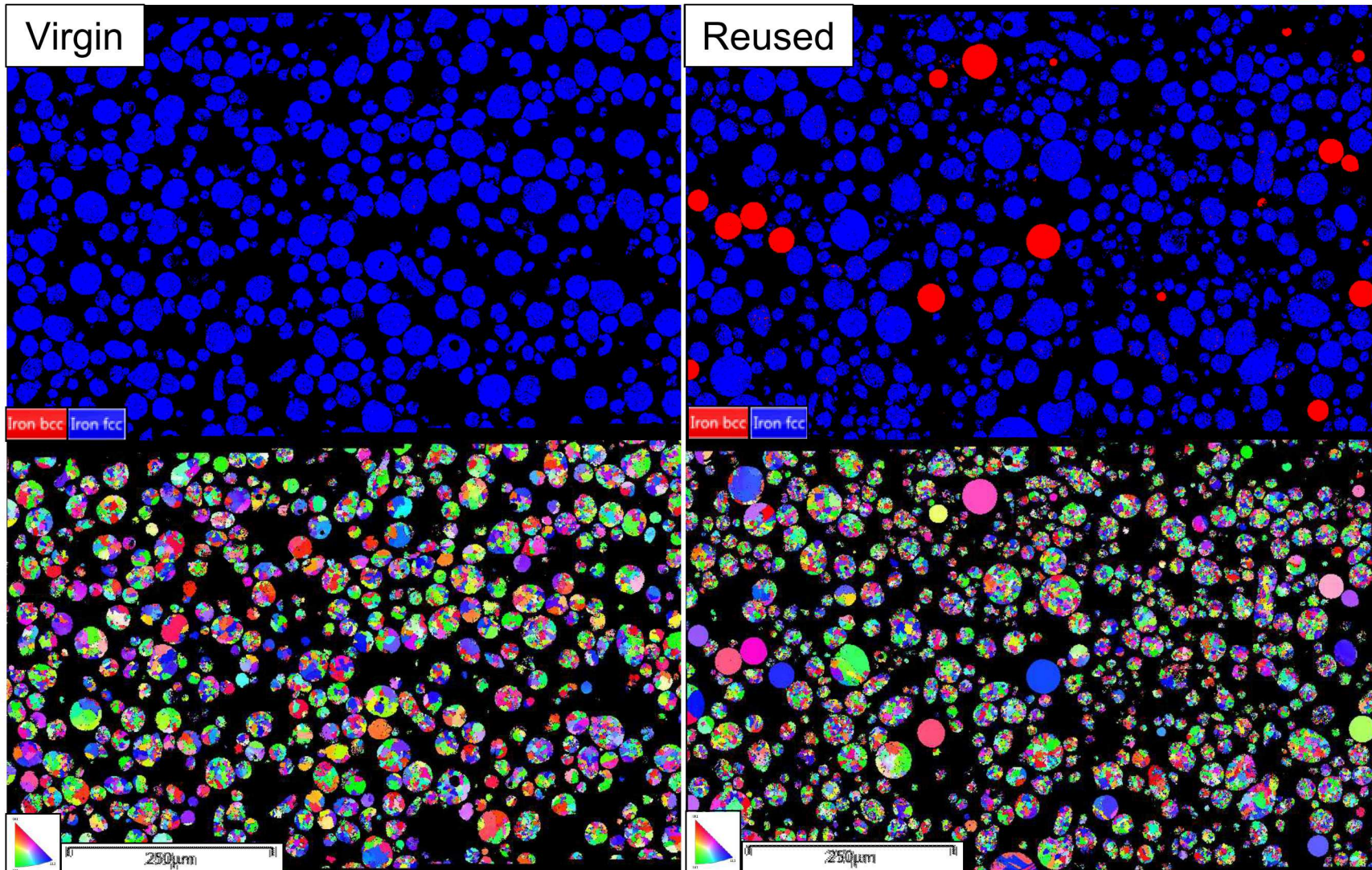
Varying levels of porosity in all powder samples



- Some reused particles contained no grain boundaries
- Slight reduction in true particle density

Powder Sample	True Particle Density (g/cm ³)
Virgin	7.922 (0.005)
Reused	7.893 (0.005)

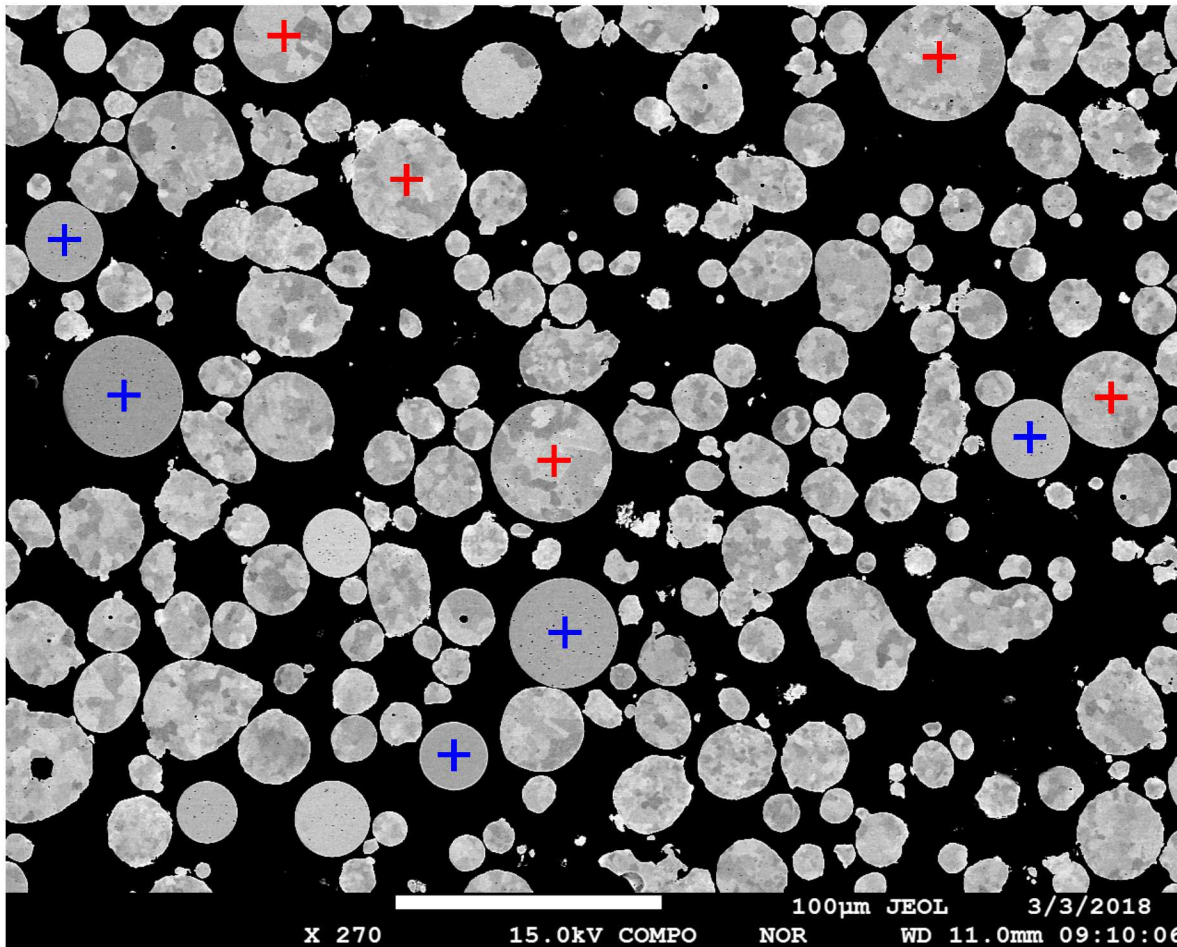
Single crystal δ ferrite particles form with reuse



Powder (Stdev)	Grain Size (μm)	Min (μm)	Max (μm)	Iron BCC (%)	Iron FCC (%)
Virgin	4.0 (2.8)	1.8	32.3	0.30	99.70
Reused	3.3 (2.1)	1.8	46.5	6.79	93.21

- Powder predominantly austenitic
- What is the origin of single crystal ferrite particles?

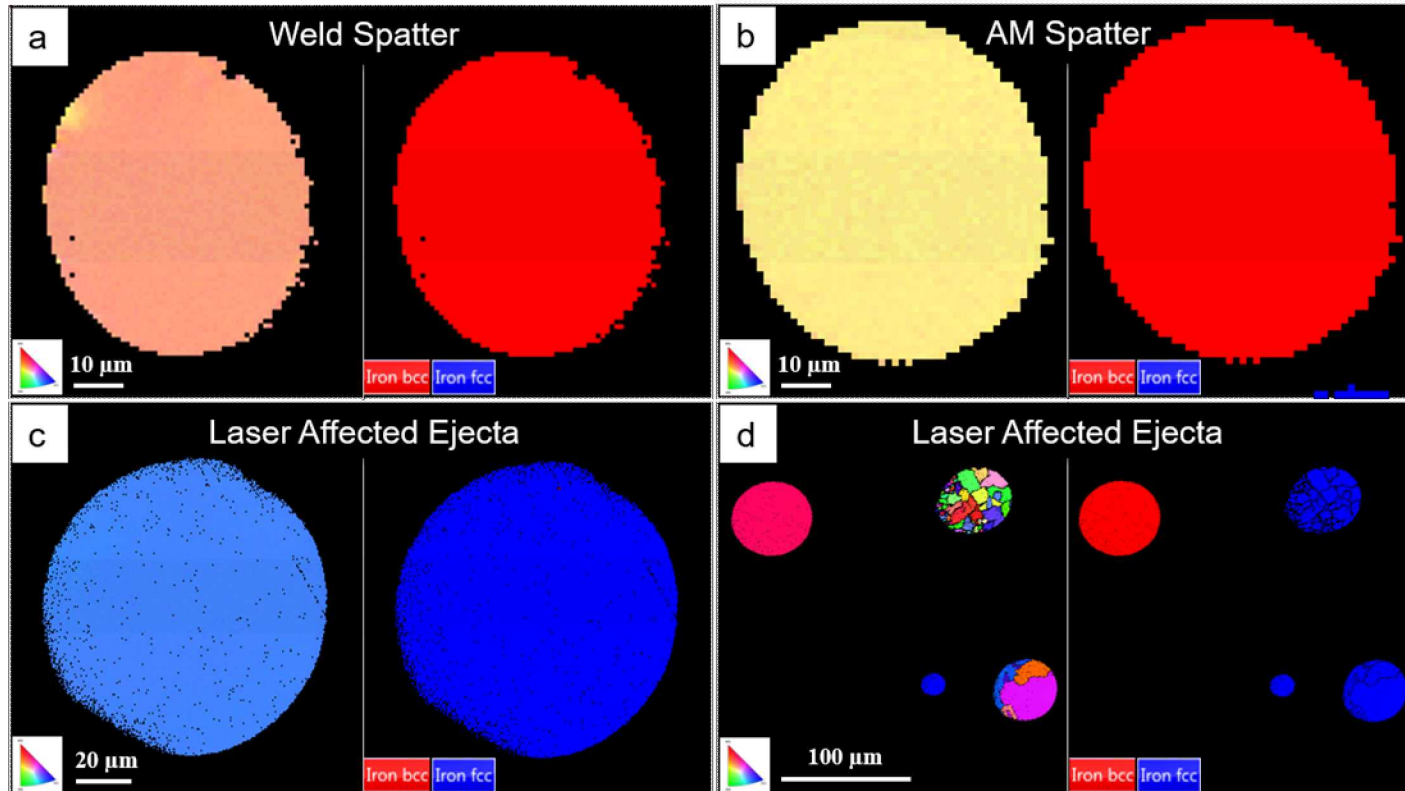
No major composition changes between polycrystalline and single crystal particles



- WDS microprobe showed that reused particles had slightly more Cr and lower Ni content than virgin state
- Cr/Ni equivalencies doesn't deviate much between polycrystalline and single crystal states
- WDS suggests single crystal formation is not compositionally driven

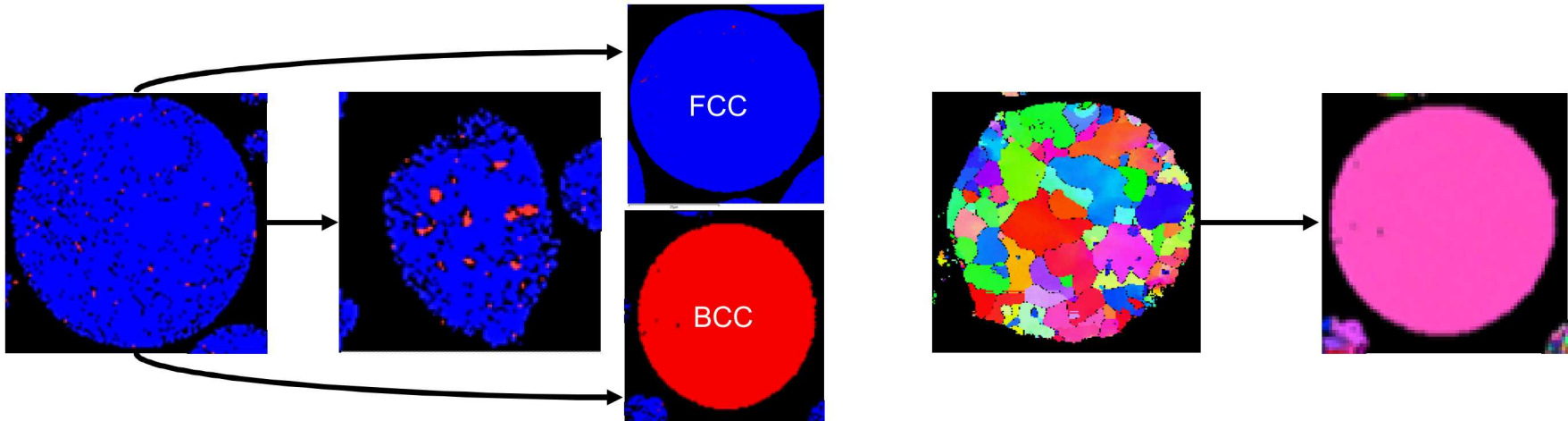
Average wt. %	Si	Mo	Mn	Ni	Cr	Fe
Virgin particle	0.65	2.05	1.20	10.81	16.84	67.80
Single Grain 	0.50	2.16	1.00	10.46	17.52	68.36
Polycrystalline 	0.58	1.98	1.28	10.65	17.49	68.03

Single crystals are the result of spatter generated from both AM melt pool and gas entrainment



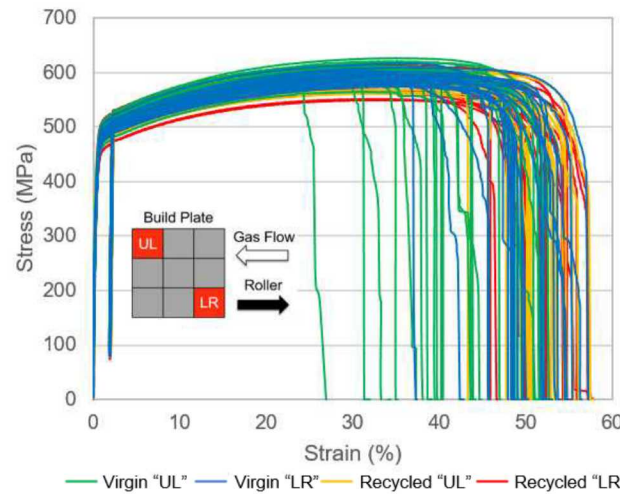
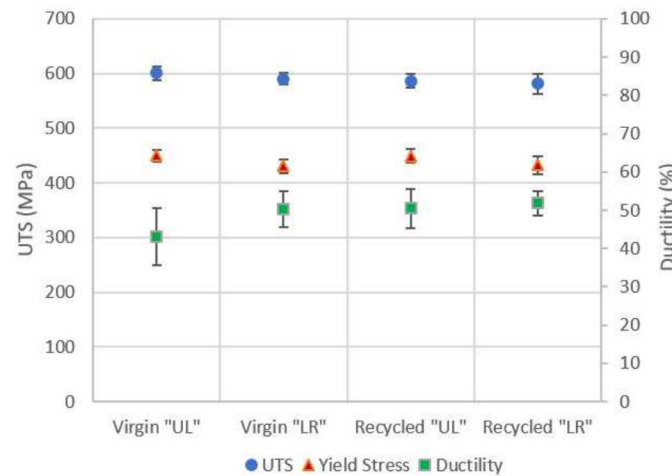
- (a) Separate weld pool experiment from two adjoining plates used to simulate melt pool particle generation – results in single crystal ferrite like (b) AM spatter
- (c & d) Pulsed laser was passed over loose powder particles to investigate changes to morphology during gas entrainment – results in same results, including single crystal austenite

Single crystal formation due to massive solidification and supercooling

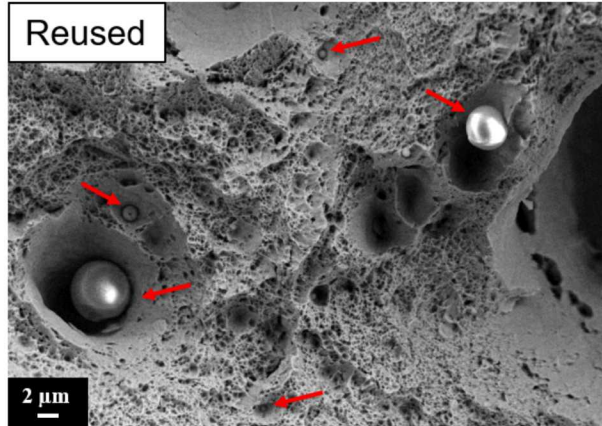
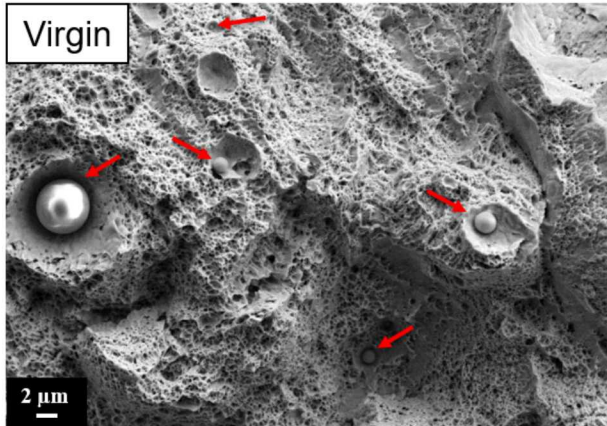


- Austenite is the primary crystallization phase of 316L stainless steel
- Kelly et al. and Cohen et al. show similar single crystal ferrite in atomized 303 depending on particle size which dictates undercooling before nucleation, and nucleation density
- For smaller metal droplets ($< 70 \mu\text{m}$) that undergo massive solidification through supercooling ($>10^5 \text{ K/s}$), noncellular, single crystal BCC can form
- Cooling rate required to achieve massive solidification becomes less drastic with decreasing number and potency of the heterogeneous nucleation sites.
- For greater liquid supercoolings, it is possible that FCC can solidify massively, but the reason for this is not clearly understood

Limited change to the part mechanical properties with 30x reuses



Powder Sample	UTS (MPa)	Yield Stress (MPa)	Elongation (%)
Virgin (UL)	600 (13)	450 (10)	43 (7)
Virgin (LR)	590 (11)	430 (13)	50 (5)
Reused (UL)	587 (12)	449 (12)	50 (5)
Reused (LR)	582 (19)	433 (17)	52 (3)

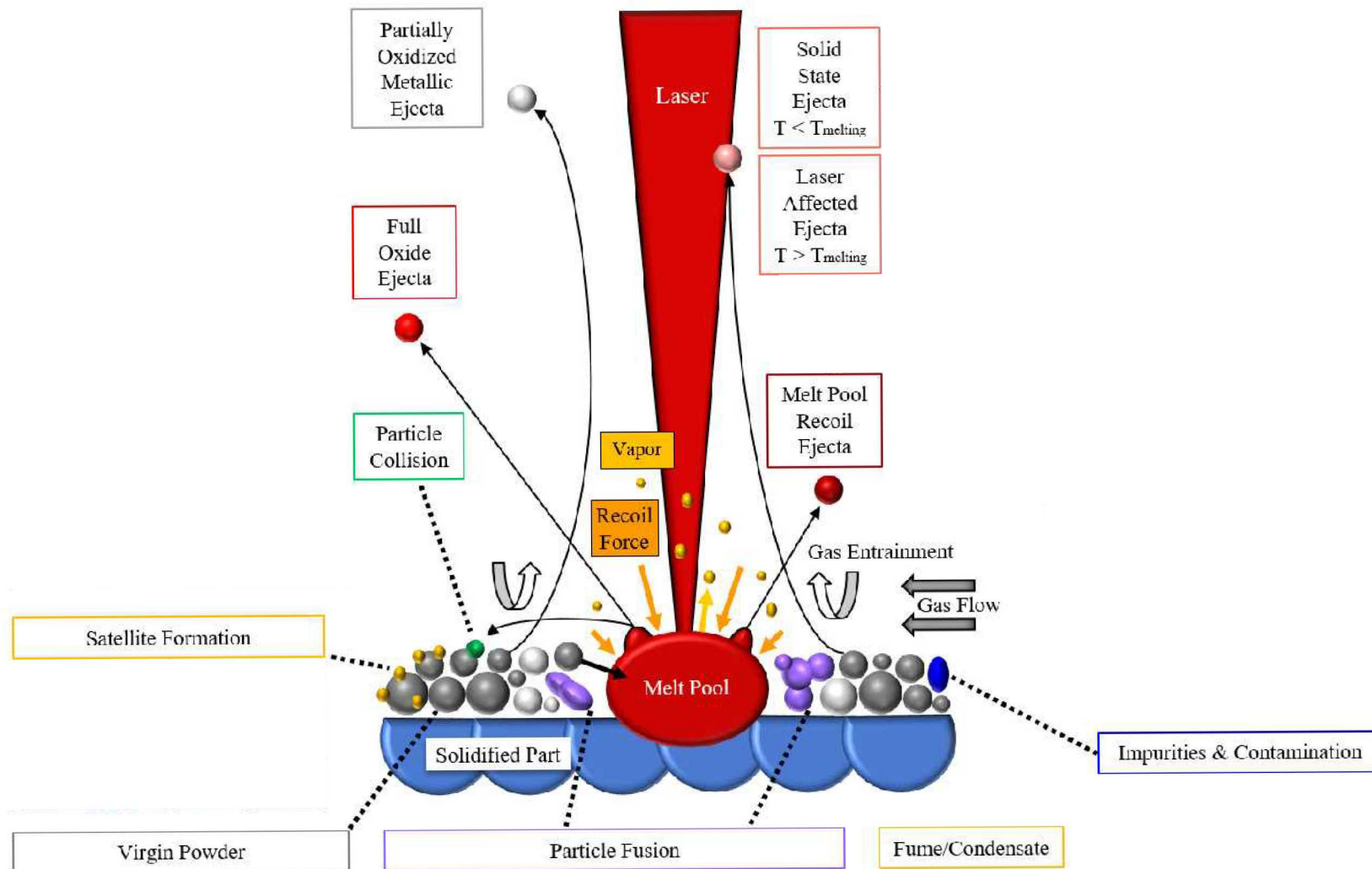


Virgin: 7.90 g/cm³
(98.72% density)

Reused: 7.81 g/cm³
(97.65% density)

- Location on build plate appears to play more of a role in affecting properties than reuse state for 316L
- However, virgin powder-built parts tend to have more variable ductility

Despite significant changes to powder properties with reuse, 316L powder is fairly robust to reuse



Acknowledgements

- Ana Baca
- Mike Brumbach
- Rebecca Chow
- Jeff Reich
- Mark Rodriguez
- Christina Profazi
- Ping Lu
- Lisa Lowery
- Tod Monson
- Charles Pearce
- Sara Dickens
- Harlan Brown-Shacklee
- James Griego
- Chris DiAntonio
- Julie Gibson
- Thomas Diebold
- Jay Carroll
- Dick Grant
- Alexander Barr
- Matthew Vieira
- Richard Grant
- Joe Michael
- Todd Huber

Paper: (Under Review)

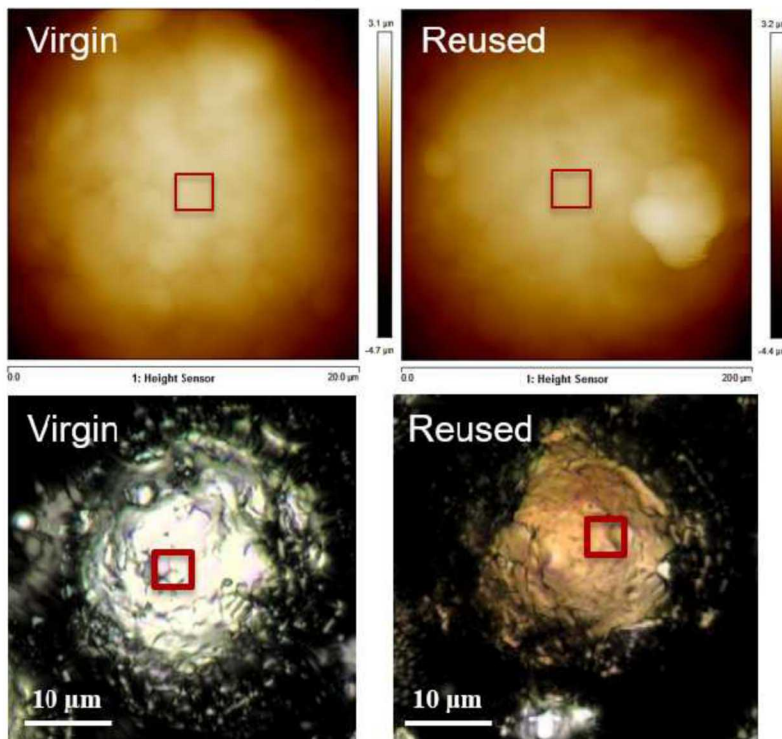
M. Heiden, L. Deibler, J. Rodelas, J. Koepke, D. Tung, D. Saiz, B. Jared, Evolution of 316L Stainless Steel Feedstock Due to Laser Powder Bed Fusion Process. Additive Manufacturing.

Appendix: Characterization Methods

Property Measured	Metrology Methods Employed
Particle size distribution	Cross section/optical microscopy, scanning electron microscopy (SEM), x-ray micro-computed tomography (μ CT), laser diffraction
Aspect ratio	Cross section/optical microscopy, SEM, μ CT
Circularity	Cross section/optical microscopy, SEM, μ CT
Internal porosity	Cross section/microscopy, SEM, μ CT
True particle density	Helium pycnometry
Grain size	Cross section/etching, SEM/EBSD, transmission electron microscopy (TEM)
Crystal structure/phase	X-ray diffraction (XRD), SEM/EBSD, TEM
Oxide thickness	TEM
Hardness	Nanoindentation
Magnetic susceptibility/coercivity	Vibrating sample magnetometer (VSM)
Bulk composition	Inductively coupled plasma mass spectrometry (ICP-MS), SEM/EDS, electron microprobe analyzer (EMPA)
Surface composition	Auger spectroscopy, x-ray photoelectron spectroscopy (XPS)
Surface Roughness	Atomic force microscopy (AFM), confocal laser scanning microscopy

Surface Finish – AFM and Confocal

AFM analysis area: $5 \mu\text{m}^2$

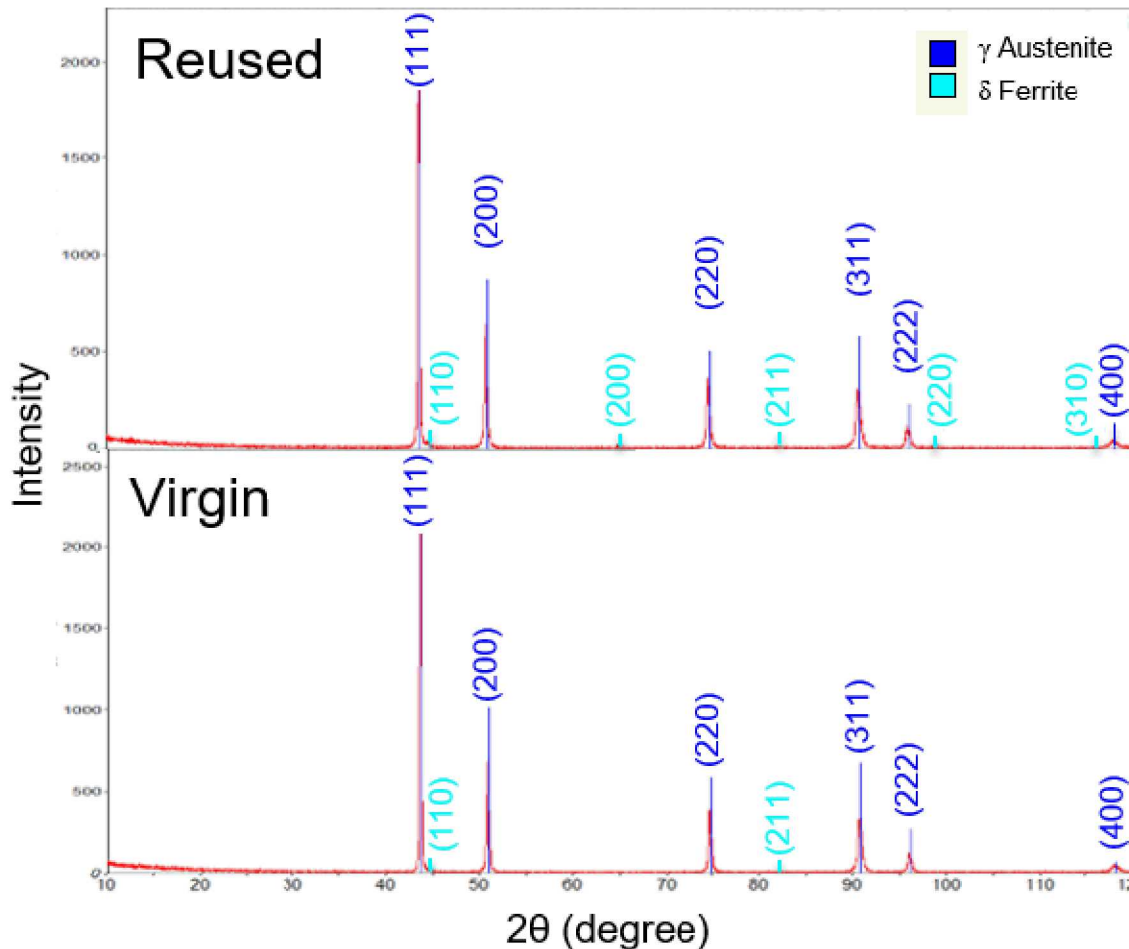


Confocal Microscope analysis area: $20 \mu\text{m}^2$

- Curvature corrections applied to both techniques
- Larger “macroscale” roughness with reuse; higher amount of satellites
- Virgin particles have higher “underlying” roughness, due to dendritic grooves
- Reused particles have better surface finish; may be from deformation or heat treatment during laser process

Average Surface Roughness S_a (Stdev)	Confocal Microscopy (Including Satellites) (nm)	AFM (Between Satellites) (nm)
Virgin	127 (53)	23 (9)
Reused	135 (66)	10 (7)

X-ray Diffraction

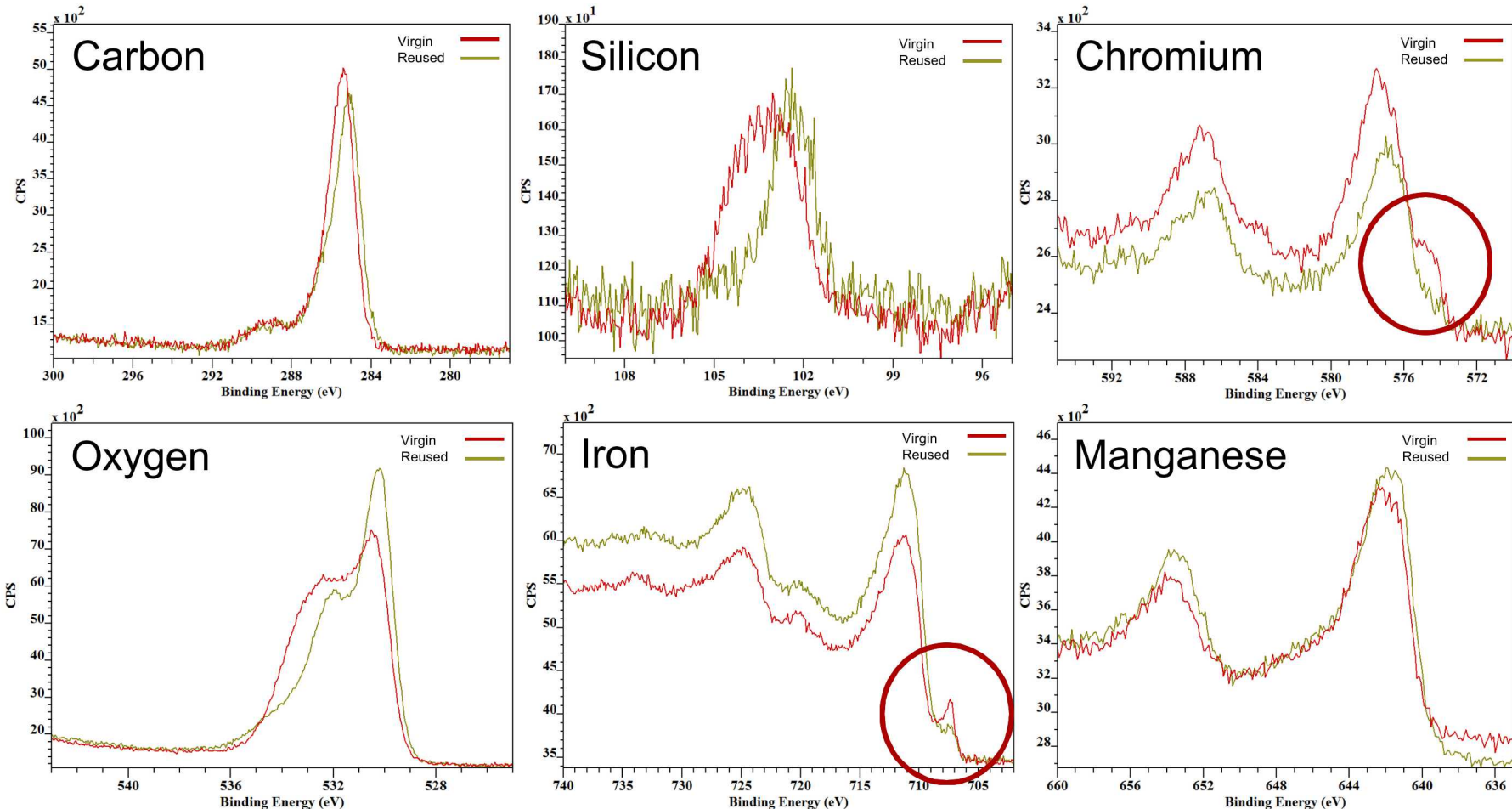


- Virgin: γ (FCC) austenite phase, with 0.5% δ (BCC) ferrite phase
- Reused: γ (FCC) austenite phase, with 1.6% δ (BCC) ferrite phase

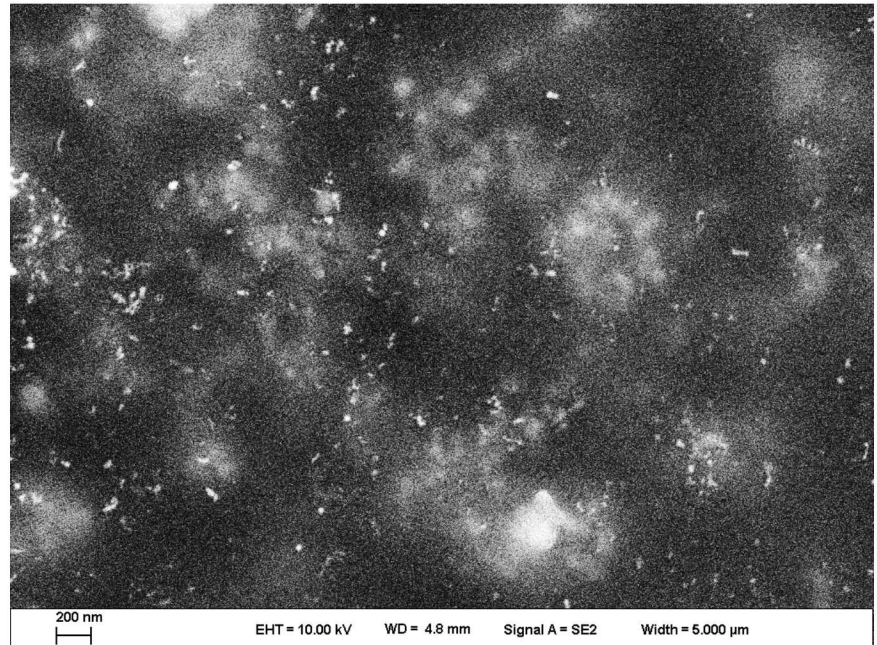
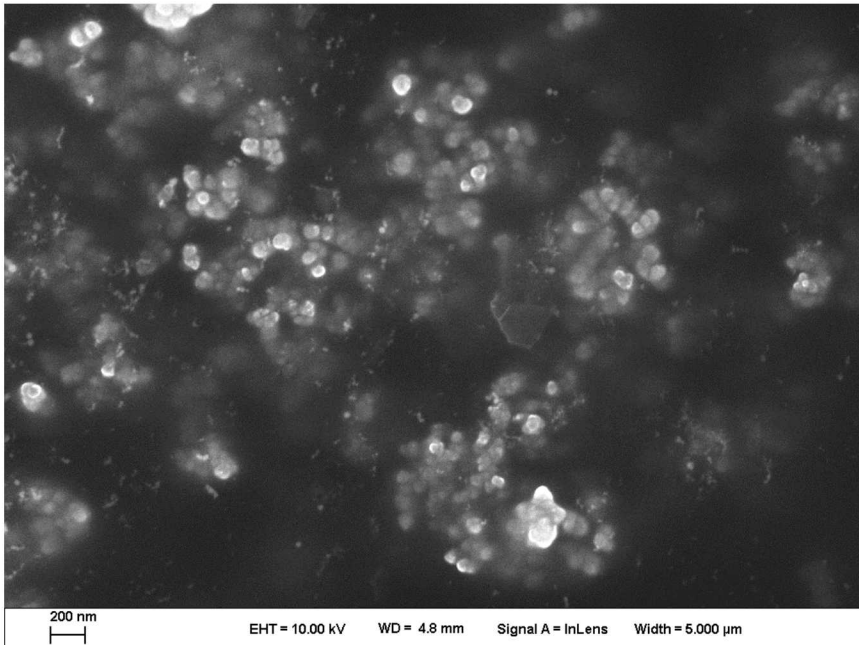
Surface Composition - XPS

Wt. % (Stdev)	O	C	Fe	Si	Mn	Cr	N	S
Virgin	33.1 (0.4)	15.3 (0.8)	25.4 (2.0)	9.3 (0.4)	9.3 (0.5)	6.7 (0.2)	0.4 (0.3)	0.4 (0.1)
Reused	30.4 (0.1)	17.6 (0.4)	29.1 (1.2)	6.4 (0.4)	11.5 (0.5)	3.9 (0.0)	0.4 (0.0)	0.7 (0.1)

- Metallic component peaks for Fe (708-708 eV) and Cr (574-575 eV) reduced with reuse
- Suggests thicker oxide



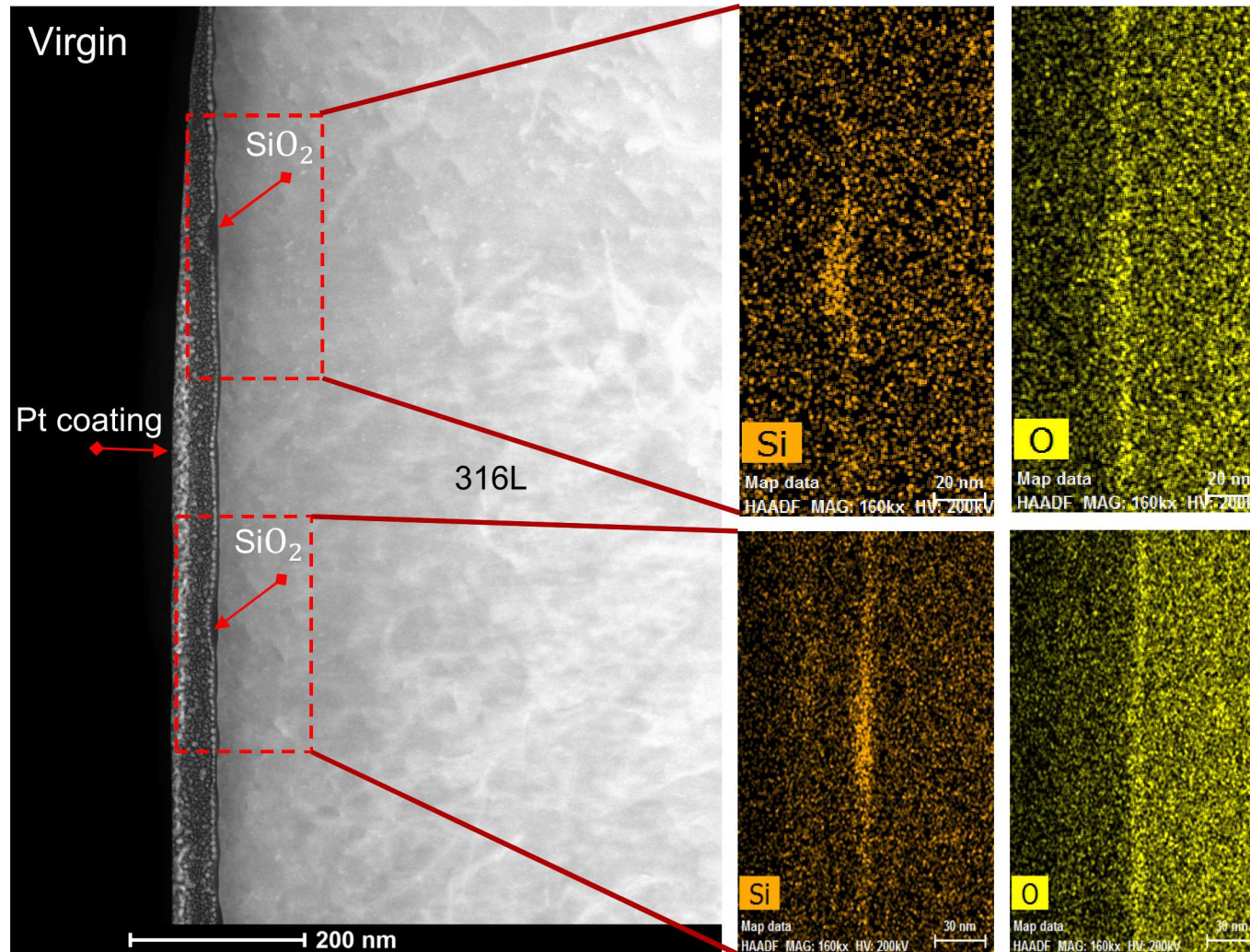
Particle Size Comparisons



Powder (Stdev)	Larger Fume (nm)	Ultrafine Fume (nm)	Wall Spatter (μ m)	Sieved (μ m)	AM Spatter (μ m)	Weld Spatter (μ m)
Average	77.8	29.8	20.9	33.6	33.5	124.3
Diameter	(18.7)	(9.0)	(9.3)	(18.1)	(14.6)	(45.3)
Max	138.0	49.8	54.1	101.6	72.5	226.5
Min	47.9	12.4	4.2	5.6	4.0	52.7

- Fume is hierarchical in nature
- One source of satellite formation and laser muting of machine lens

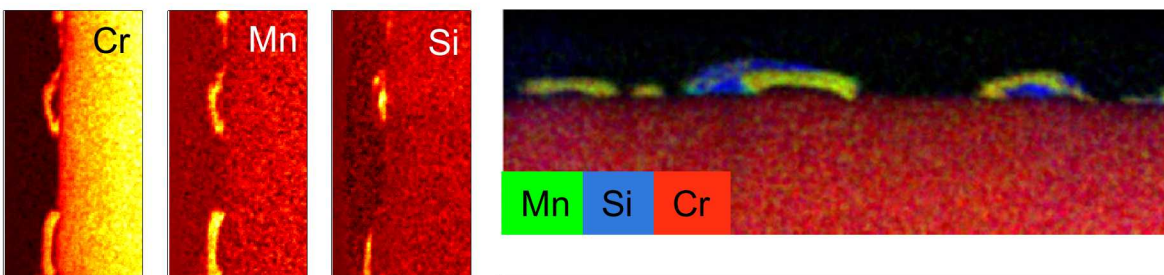
Oxide Thickness - TEM



- Virgin oxide layer is composed of SiO_2
- Average oxide thickness is $\sim 3\text{-}4\text{ nm}$
- Thicker $\sim 15\text{ nm}$ nodules tend to form near the end of grain boundaries

Oxide Thickness - TEM

Reused



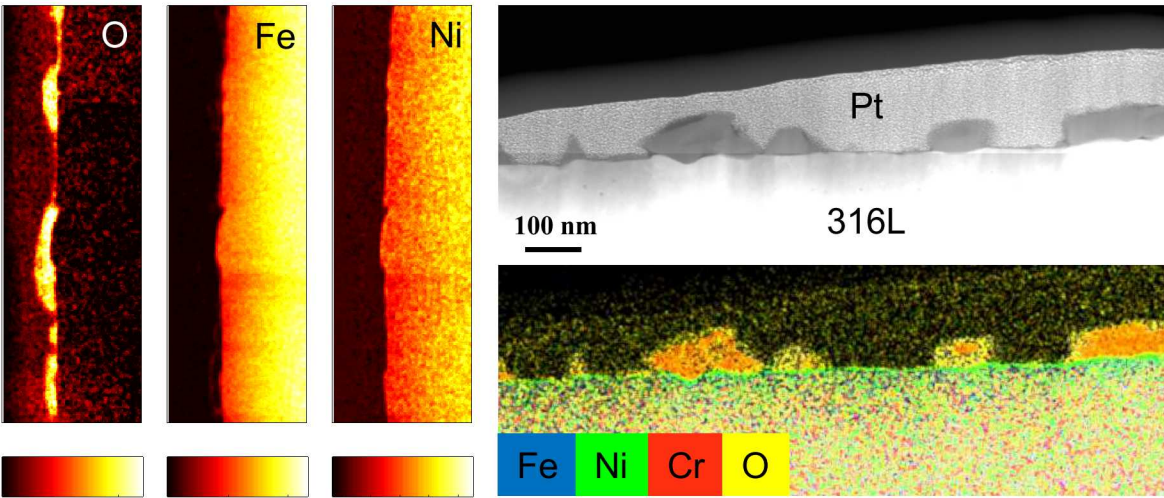
Pt 316L



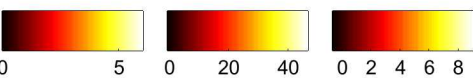
MnCr_2O_4

SiO_2

HAADF



Map data 200 nm
HAADF MAG: 20.0k



- Reused particles form MnCr_2O_4 and larger SiO_2 nodules across the surface
- Mn and Cr depleted zone beneath the oxide layer

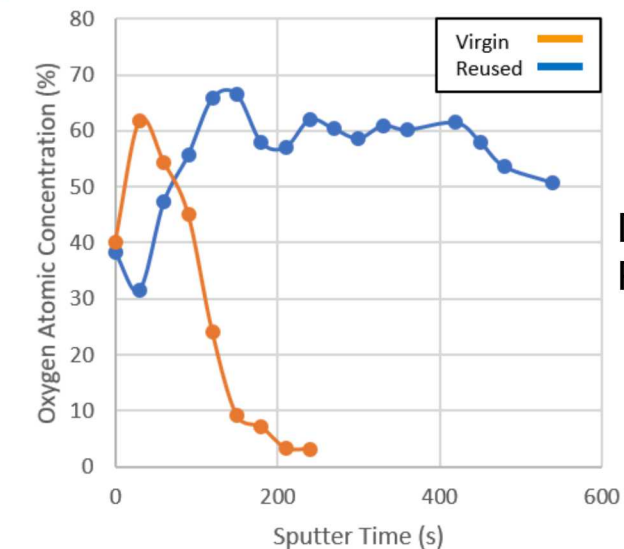
Surface Composition - Auger

Irregular, characteristically rough particles								
Wt. % (Stdev)	O	C	Fe	Si	Mn	Cr	Ni	S
Virgin	23.2 (5.1)	9.7 (1.0)	41.9 (5.5)	6.0 (2.3)	-	15.8 (9.1)	3.0 (1.7)	0.4 (0.2)
	34.2 (3.0)	12.2 (4.4)	38.2 (3.7)	9.9 (2.6)	-	-	4.7 (2.4)	0.8 (0.1)
Round, characteristically smooth particles								
Wt. % (Stdev)	O	C	Fe	Si	Mn	Cr	Ni	S
Virgin	30.5 (2.8)	6.2 (1.0)	52.8 (7.0)	10.5 (5.9)	-	-	-	-
	22.4 (3.7)	5.9 (2.7)	28.5 (2.0)	18.7 (1.5)	24.5 (1.4)	-	-	-

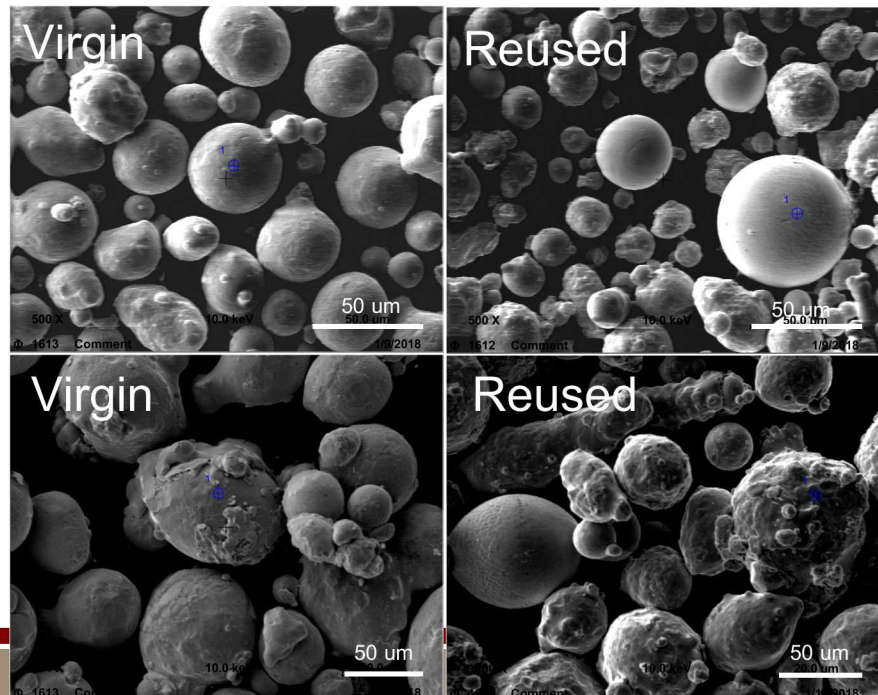
- C, Si, Mn increased for smooth
- O, Si, Ni, S increased for rough
- Depth profiling showed increase in oxide thickness with reuse

Round

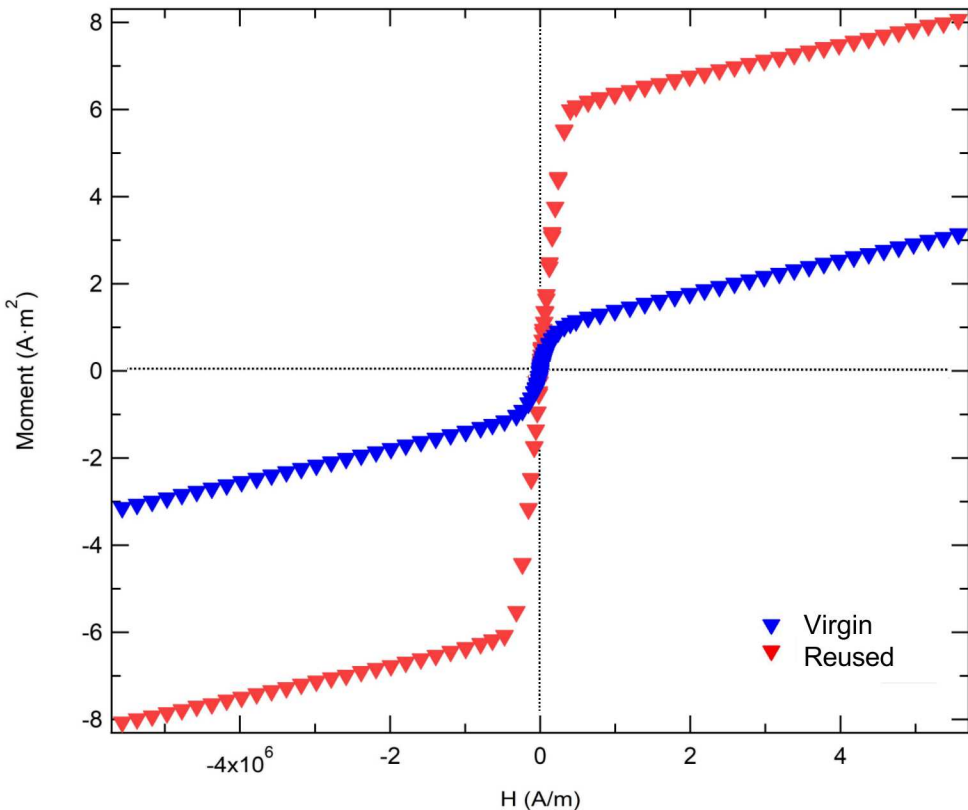
Irregular



Depth Profiling



Magnetic Susceptibility

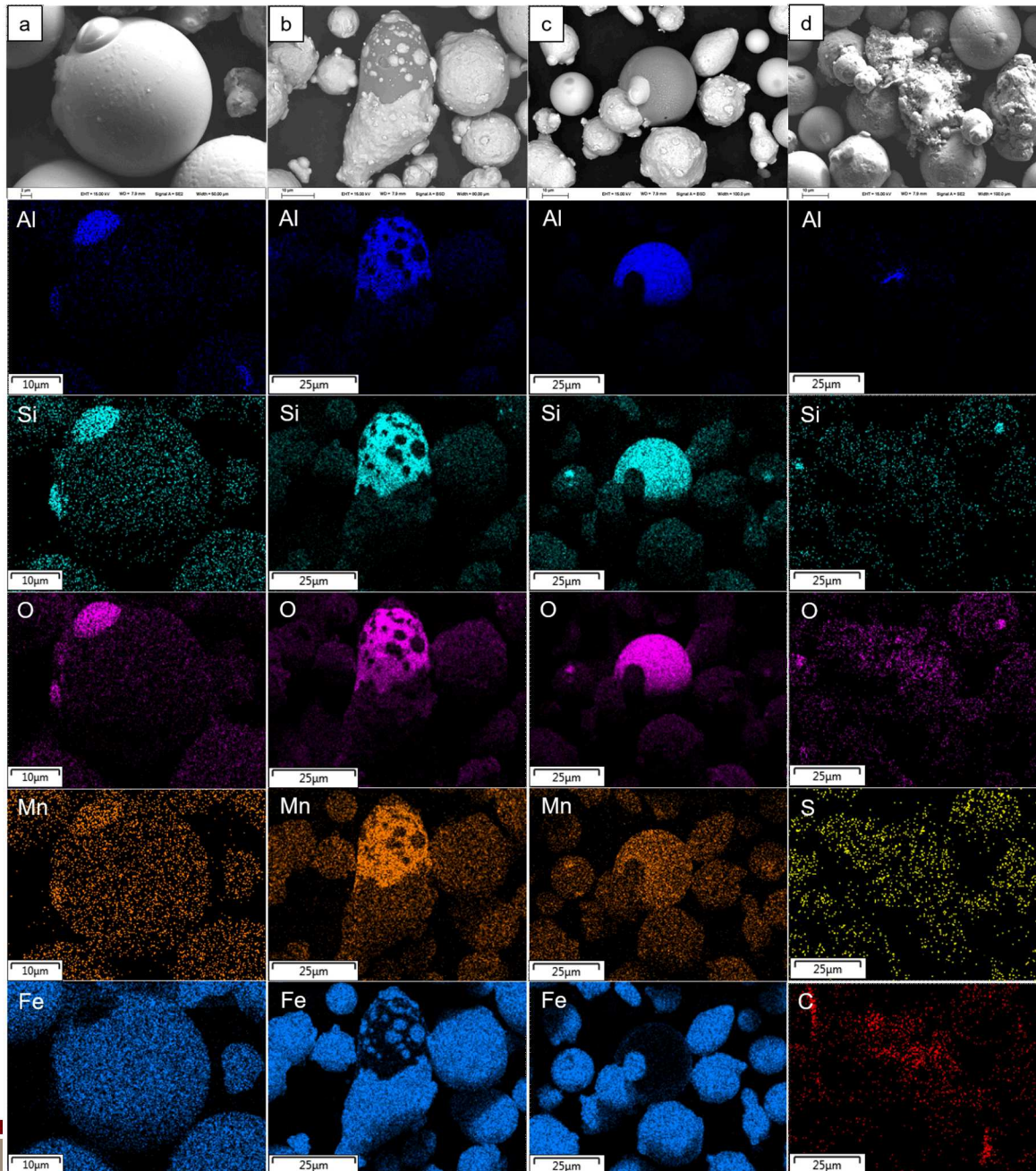


- Significant increase in magnetic susceptibility of reused powder
- Reused powder has a higher max magnetic moment (strength of magnetization)
- Virgin power has a higher coercivity; harder to demagnetize

Powder Sample	Moment at 7T (Am ² /kg)	Coercivity (A/m)	Susceptibility
Virgin	3.137	4651.53	7.07E-06 (2.89E-07)
Reused	8.065	1383.80	2.38E-05 (3.84E-07)

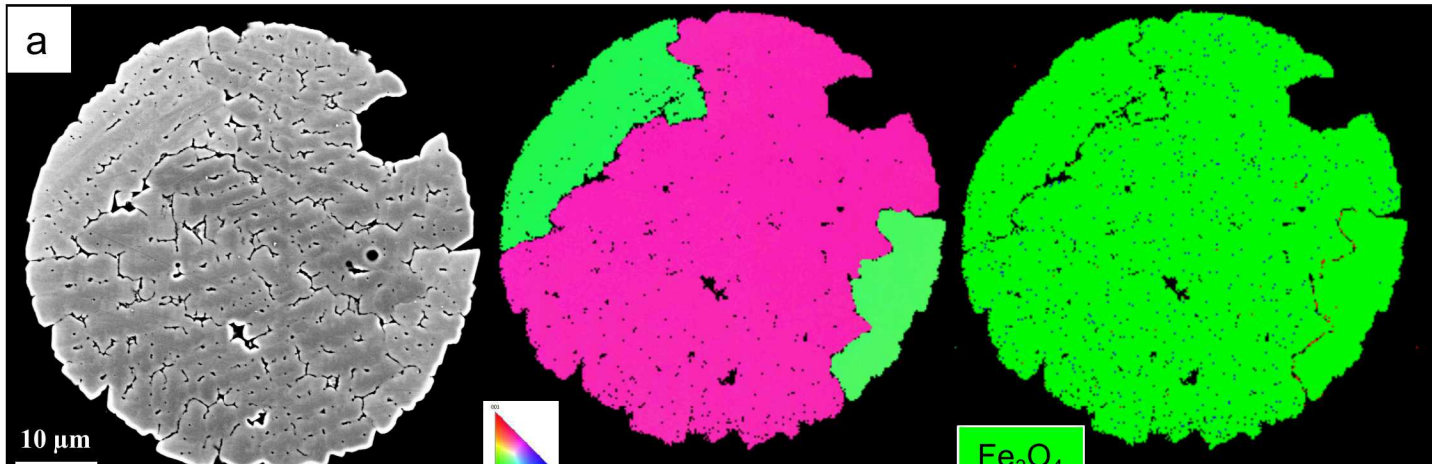
$$\chi_m = \frac{M}{H}$$

Wall-Condensate



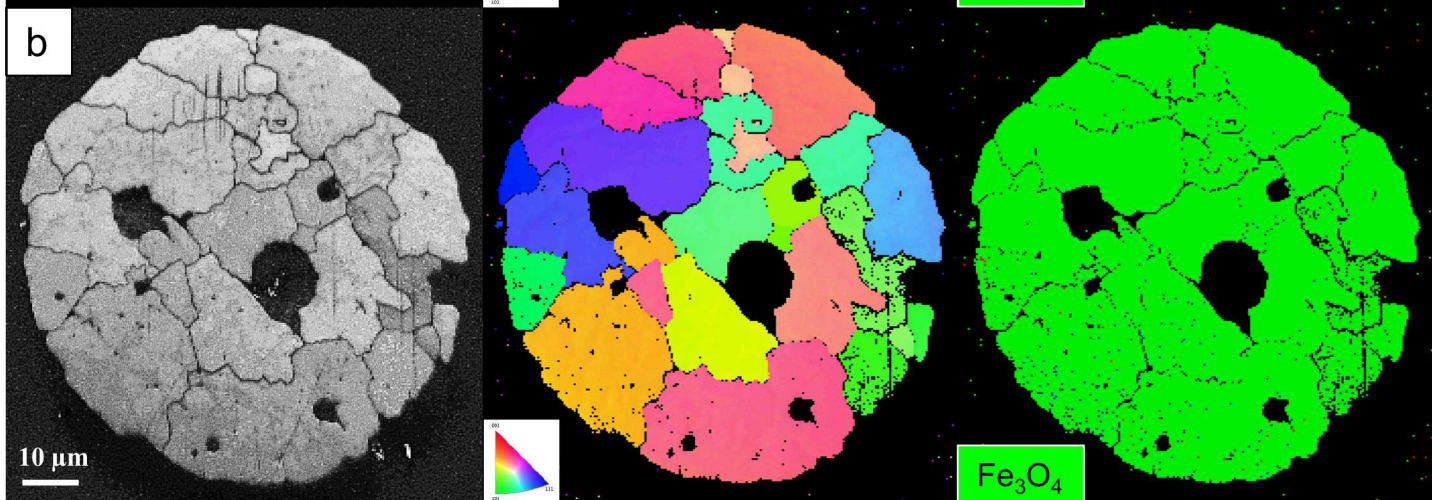
- Powder found on the walls of the AM chamber tend to contain Al oxide impurities and soot from the process
- Si and Mn oxide particle formations common
- Particle sizes are similar to regular sputter

Weld
Spatter
Oxide



Oxide

AM
Spatter
Oxide



Fe₃O₄: 98.84%
Fcc: 0.96%
Bcc: 0.20%

EDS
Weld
Spatter

